

Significant Improvement in Superconductivity by Substituting Pb at Bi-site in $\text{Bi}_{2-x}\text{Pb}_x\text{Sr}_2\text{CaCu}_2\text{O}_8$ with $x = 0.0$ to 0.40

Jagdish Kumar · P.K. Ahluwalia · H. Kishan ·
V.P.S. Awana

Received: 27 November 2009 / Accepted: 22 December 2009 / Published online: 23 January 2010
© Springer Science+Business Media, LLC 2010

Abstract Here we report the synthesis and superconducting properties of bulk $\text{Bi}_{2-x}\text{Pb}_x\text{Sr}_2\text{CaCu}_2\text{O}_8$ ($x = 0.0$ to 0.4) compound. Though the superconducting transition temperature (T_c) decreases marginally, the critical current density under magnetic field $J_c(H)$ increases with Pb content. An optimization is observed for $x = 0.16$ with $J_c(H)$ ($7.894 \times 10^3 \text{ A/cm}^2$) that is nearly doubled in comparison to the pristine compound. It seems that controlled substitution of Pb at Bi-site in bulk Bi-2212 ($\text{Bi}_2\text{Sr}_2\text{CaCu}_2\text{O}_8$) system can enhance the superconducting critical parameters. These results are explained on the basis of possible improved inter- and intra-granular properties with Pb substitution in $\text{Bi}_{2-x}\text{Pb}_x\text{Sr}_2\text{CaCu}_2\text{O}_8$ system.

Keywords Bi-2212 ($\text{Bi}_2\text{Sr}_2\text{CaCu}_2\text{O}_8$) system · Superconducting transition temperature (T_c) · Critical current density and magnetization

1 Introduction

High-temperature superconductivity has been one of greatest achievements of the experimental physics. Among various high-temperature superconductors (HTSc), cuprates share many common features in layered crystal structure and properties. Cava [2] has proposed a local charge picture in understanding the relative change in superconducting properties with layered crystal structure of cuprates. According

to this local charge picture, all the layered cuprate superconductors are considered to be built up of superconducting CuO_2 layers. These layers are sandwiched between other structural layers which act as spacers as well as electronic charge reservoirs. The doping of superconducting CuO_2 layers is controlled by the electronic state of charge reservoirs. In high- T_c superconducting compounds, the superconductivity is obtained by doping (adding charge carriers) to the CuO_2 layers. The cation substitutions can change the effective copper valence and the carrier concentration which is strongly linked with T_c .

Like other high- T_c cuprates, $\text{Bi}_2\text{Sr}_2\text{Ca}_{n-1}\text{Cu}_n\text{O}_{2n+4+\delta}$ (BSCCO) compounds have layered crystal structure with alternating rock-salt and perovskite blocks. These blocks constitute a homologous system with superconducting transition temperature (T_c^{\max}) = 20, 85 and 110 K corresponding to $n = 1, 2$ and 3 [1]. Like other cuprates, two-dimensional CuO_2 layers act as superconducting planes, and other $\text{Bi}_2\text{O}_{2+\delta}$ provide charge carriers for the CuO_2 planes in BSCCO. Among various BSCCO superconductors, Bi-2212 ($n = 1$) has been found as the most approved and suitable to serve as wires in magnetic applications because of its chemical stability and manufacturing flexibility. However, one of the serious problems associated with Bi-2212 is its critical current density (J_c) which decreases drastically in magnetic field. This decrease originates from the breakdown of the zero resistive state due to thermally activated flux flow. Partial replacement of Bi^{3+} by Pb^{2+} in $\text{Bi}_2\text{Sr}_2\text{CaCu}_2\text{O}_{8+\delta}$ (Bi-2212) is known to enhance significantly the superconducting critical parameters. It is known to suppresses the c -axis component of the modulation [3, 4], reduce anisotropy, improve intra-granular pinning properties [5] and invoke a better coupling of superconductivity $\text{Cu}-\text{O}_2$ planes in c -direction through SNS (superconducting-normal-superconducting) junctions [6].

J. Kumar · H. Kishan · V.P.S. Awana (✉)
National Physical Laboratory (CSIR), Dr. K.S. Krishnan Marg,
New Delhi, 110012, India
e-mail: awana@mail.nplindia.ernet.in

J. Kumar · P.K. Ahluwalia
Himachal Pradesh University, Shimla, 171005, HP, India

In present work we have synthesized a series of bulk $\text{Bi}_{2-x}\text{Pb}_x\text{Sr}_2\text{CaCu}_2\text{O}_8$ with Pb substitution from $x = 0.0$ to 0.4 at Bi-site, and have found significant improvement in the superconducting properties for an optimal value of $x = 0.16$. Further, we conclude that although we used a different synthesis procedure to obtain T_c^{\max} of above 92 K for pristine sample, the impact of Pb substitution is the same as reported earlier for $\text{Bi}_{2-x}\text{Pb}_x\text{Sr}_2\text{CaCu}_2\text{O}_8$ [4–6] single crystals or differently processed Bi-2212. It is worth mentioning that for large-scale applications, i.e., wires, tapes, etc., large bulk quantities of the material are required, instead of tiny crystals. Keeping this in view, the present study on bulk $\text{Bi}_{2-x}\text{Pb}_x\text{Sr}_2\text{CaCu}_2\text{O}_8$ is carried out and optimization of its superconducting performance is achieved.

2 Experimental

The titular sample series of $\text{Bi}_{2-x}\text{Pb}_x\text{Sr}_2\text{CaCu}_2\text{O}_{8+\delta}$ ($x = 0$ to 0.4) were prepared by conventional solid-state reaction method. The starting raw powdered materials with high purity of Bi_2O_3 , SrCO_3 , CaCO_3 , PbO and CuO were mixed in appropriate ratios as required for an overall 2212 stoichiometry. The grounded homogeneous powders were calcined at 800°C for 12 hours. The sample powders were then annealed in air at 820°C , 840°C and 850°C consequently for 24 hours with intermediate regrinding. Finally, grinded powders were pressed into pellets under a pressure of 100 Kg/cm^2 and partially melted at 930°C for a few minutes and again annealed in air at 860°C for 24 hours. Then they were quenched to room temperature and finally annealed in N_2 atmosphere at 650°C to optimize the transition temperature (T_c) [7] by controlling the oxygen content. The room temperature X-ray powder diffraction patterns were recorded with Cu-K_α radiation using Rigaku Miniflex-II table top diffractometer. The phase purity and lattice parameter refining were done by indexing peaks corresponding to Bi-2212 [8] structure. Magnetic measurements were carried out using SQUID magnetometer. $R(T)$ measurements were carried out by standard four-probe technique. Also SEM images of the samples were taken to study the microstructure.

3 Results

Figure 1 depicts the room temperature X-ray diffraction (XRD) patterns of $\text{Bi}_{2-x}\text{Pb}_x\text{Sr}_2\text{CaCu}_2\text{O}_8$ ($x = 0.0$ to 0.4) samples. The peak indexing of the X-ray diffractograms confirmed that all the samples contain Bi-2212 as the main phase. However, a little impurity peaks of Bi-2201 ($2\theta = 29.64^\circ$ maximum intensity peak) [9] and $\text{Bi}_{0.96}\text{Pb}_{0.24}\text{SrCaCu}_{1.5}\text{O}_{5+x}$ ($2\theta = 36.64^\circ$) [10] and that of

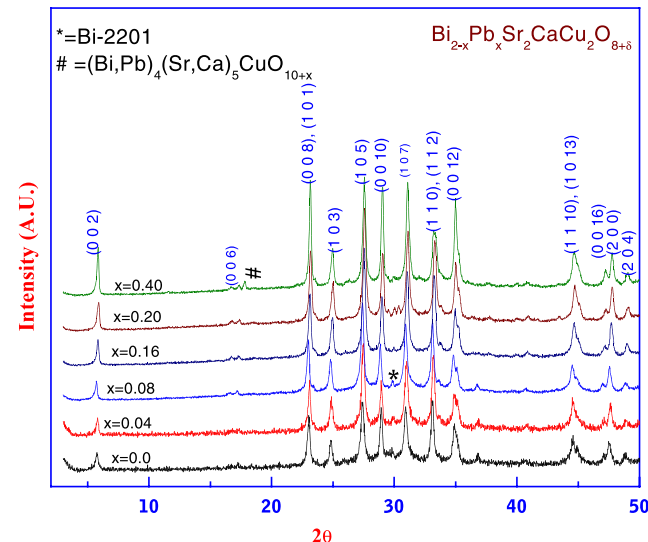


Fig. 1 XRD pattern of $\text{Bi}_{2-x}\text{Pb}_x\text{Sr}_2\text{CaCu}_2\text{O}_{8+\delta}$ ($x = 0$ to 0.4)

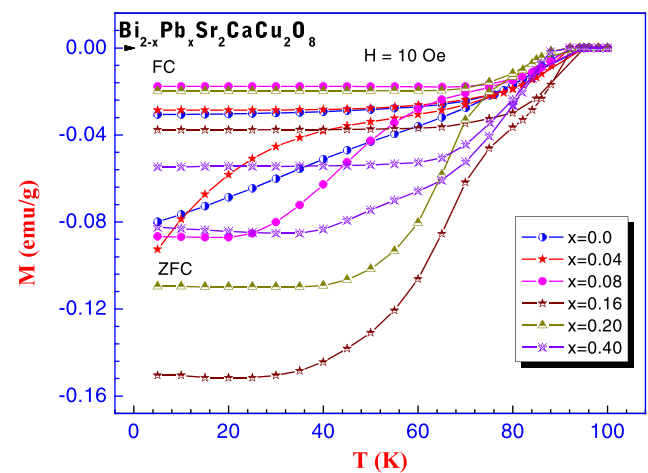


Fig. 2 Magnetic moment in FC and ZFC for $\text{Bi}_{2-x}\text{Pb}_x\text{Sr}_2\text{CaCu}_2\text{O}_{8+\delta}$ ($x = 0$ to 0.4)

$(\text{Bi},\text{Pb})_4(\text{Sr},\text{Ca})_5\text{CuO}_{10+x}$ [11] were observed. The sample with $x = 0.16$ however shows comparatively lesser impurity peaks. The calculated lattice parameters of the $\text{Bi}_{2-x}\text{Pb}_x\text{Sr}_2\text{CaCu}_2\text{O}_8$ samples with $x = 0.0$ to 0.4 are given in Table 1.

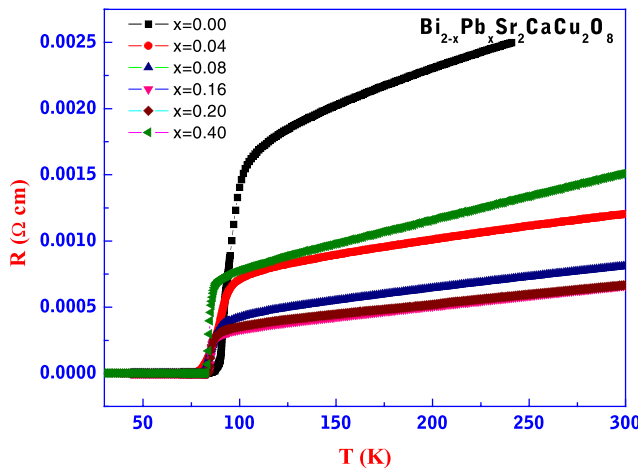
The magnetization vs. temperature measurements are shown in Fig. 2 for an applied magnetic field of 10 Oe in both the cases, i.e. field-cooled (FC) and zero-field-cooled (ZFC), using SQUID magnetometer. From these measurements we can see that the T_c^{Dia} onset value is almost the same for all the samples ($T_c^{\text{Dia}} \simeq 92$ K). A large hysteresis is observed below the irreversible temperature T_{irr} at which the zero-field-cooled (ZFC) and the field-cooled (FC) branches coincide. The splitting of FC and ZFC curves improves up to $x = 0.16$ and then it starts to deteriorate. The most interesting feature observed was the regular increase in T_{irr}

Table 1 Lattice parameters a and c for $\text{Bi}_{2-x}\text{Pb}_x\text{Sr}_2\text{CaCu}_2\text{O}_8$ samples with $x = 0.0$ to 0.4

$x \rightarrow$	0.00	0.04	0.08	0.16	0.20	0.40
a (Å)	3.825(7)	3.820(1)	3.824(3)	3.813(2)	3.807(4)	3.807(5)
c (Å)	30.531(2)	30.430(6)	30.635(8)	30.231(6)	30.035(3)	30.232(5)

Table 2 The irreversibility temperature T_{irr} (K) for $\text{Bi}_{2-x}\text{Pb}_x\text{Sr}_2\text{CaCu}_2\text{O}_8$ samples with $x = 0.0$ to 0.4

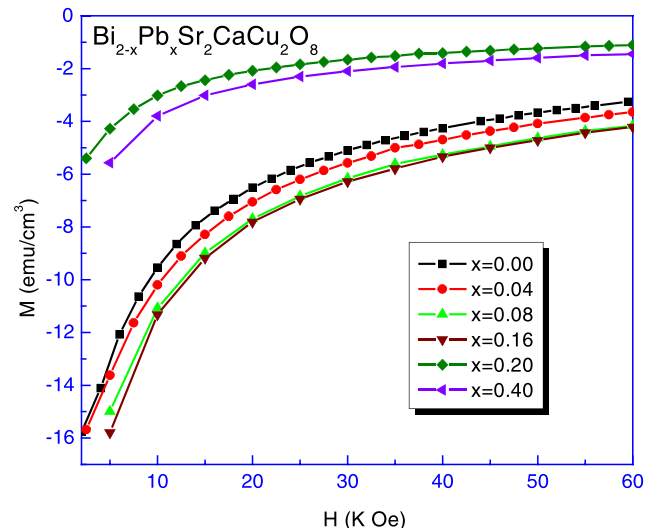
S. No.		T_{irr} (K)
1	$\text{Bi}_{2-x}\text{Pb}_x\text{Sr}_2\text{CaCu}_2\text{O}_8$	80.5
2	$\text{Bi}_{1.96}\text{Pb}_{0.04}\text{Sr}_2\text{CaCu}_2\text{O}_8$	84.13
3	$\text{Bi}_{1.92}\text{Pb}_{0.08}\text{Sr}_2\text{CaCu}_2\text{O}_8$	85.54
4	$\text{Bi}_{1.84}\text{Pb}_{0.16}\text{Sr}_2\text{CaCu}_2\text{O}_8$	88.62
5	$\text{Bi}_{1.8}\text{Pb}_{0.2}\text{Sr}_2\text{CaCu}_2\text{O}_8$	85.67
6	$\text{Bi}_{1.6}\text{Pb}_{0.4}\text{Sr}_2\text{CaCu}_2\text{O}_8$	85.02

**Fig. 3** Resistivity vs. temperature for $\text{Bi}_{2-x}\text{Pb}_x\text{Sr}_2\text{CaCu}_2\text{O}_8+\delta$ ($x = 0$ to 0.4)

with Pb content up to $x = 0.16$ with subsequent deterioration, as is summarized in Table 2. This result suggests that the Pb substitution suppresses flux flow at high temperatures and leads to an increase in critical current density (J_c) [5] in $\text{Bi}_{2-x}\text{Pb}_x\text{Sr}_2\text{CaCu}_2\text{O}_8$, up to $x = 0.16$, and then decreases for higher values of x [12] as is observed in J_c measurements.

The T_c^{Dia} onset values are in good agreement with those observed in $R-T$ measurements, as is shown in Fig. 3. We can observe from the $R-T$ curves that there is a regular decrease in the normal state resistivity (increase in conductivity) with increase in Pb content up to $x = 0.16$ with subsequent increase (decrease in conductivity) with a further increase in the value of x . There is no regularity in the $T_c^{R=0}$ with the change of Pb content, and it is around 85 K for all the samples.

The $M-H$ measurements are depicted in Fig. 4. From these measurements we can infer that there is a regular increase in magnetization with the increase in Pb con-

**Fig. 4** Magnetization ($M-H$) plots for $\text{Bi}_{2-x}\text{Pb}_x\text{Sr}_2\text{CaCu}_2\text{O}_8$ system

tent up to $x = 0.16$. However, there is a sudden degradation of diamagnetism for $x > 0.16$. The behavior of $M-H$ curves is similar in all the samples with different magnitudes.

Figure 5 shows the behavior of critical current density with applied field $J_c(H)$ of the $\text{Bi}_{2-x}\text{Pb}_x\text{Sr}_2\text{CaCu}_2\text{O}_8$ ($x = 0.00$ to 0.40) samples. The $J_{c,m}$ for all the samples at $T = 5$ K, has been observed from the measurements of the magnetic hysteresis loop as in [13]:

$$J_{c,m} = \frac{30\Delta M}{d} \text{ A/cm}^2$$

where, ΔM (A/cm²) is the width of hysteresis loop and d is the diameter of the cylindrical sample. The measurements were made with the field applied perpendicularly to the sample axis in order to obtain the current path similar to that in the transport measurements. It can be clearly seen that the value of J_c is optimal for the $x = 0.16$ sam-

ple, and then it drops with a further increase in Pb content. The optimal value of J_c has been found to be 7.894×10^3 A/cm².

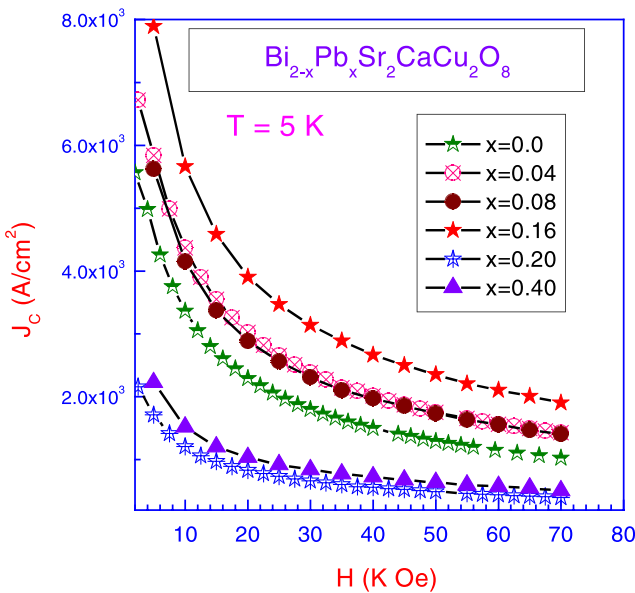


Fig. 5 J_c measurements for $\text{Bi}_{2-x}\text{Pb}_x\text{Sr}_2\text{CaCu}_2\text{O}_{8+\delta}$ ($x = 0$ to 0.4)

In Fig. 6 the $J_c(H)$ of the samples at 5 and 20 K is shown. It also shows the percentage decrease in maximal value of J_c respectively at 5 and 20 K. As can be seen from the figure, the percentage decrease in the maximal value of J_c at 5 and 20 K remains at about 70 percent of an optimized value ($x = 0.16$) in $\text{Bi}_{2-x}\text{Pb}_x\text{Sr}_2\text{CaCu}_2\text{O}_8$ and then increases to 74 and 78 percent with a further increase in x .

Figure 7 shows the SEM micrographs of the $\text{Bi}_{2-x}\text{Pb}_x\text{Sr}_2\text{CaCu}_2\text{O}_8$ samples with the same magnification (10KX). From Fig. 7 (corresponds to lead-free Bi-2212) we can see a plate-like growth of grains with random orientation. Comparing the micrographs of Pb doped and un-doped Bi-2212, we found that plate-like growth of the grains disappears, and at higher concentration of lead we obtained a needle-like grains. For $\text{Bi}_{1.60}\text{Pb}_{0.40}\text{Sr}_2\text{CaCu}_2\text{O}_8$ large needles of about $10\text{--}15 \mu\text{m}$ were observed. Moreover, the packing fraction and hence the inter-granular connectivity improves in $\text{Bi}_{2-x}\text{Pb}_x\text{Sr}_2\text{CaCu}_2\text{O}_8$ up to $x = 0.16$ and then degrades with a further increase in x . As far as secondary phases are concerned, no significant quantity of extra phases were seen in $\text{Bi}_{2-x}\text{Pb}_x\text{Sr}_2\text{CaCu}_2\text{O}_8$ samples up to $x = 0.16$. However, some amounts of extra phases were seen

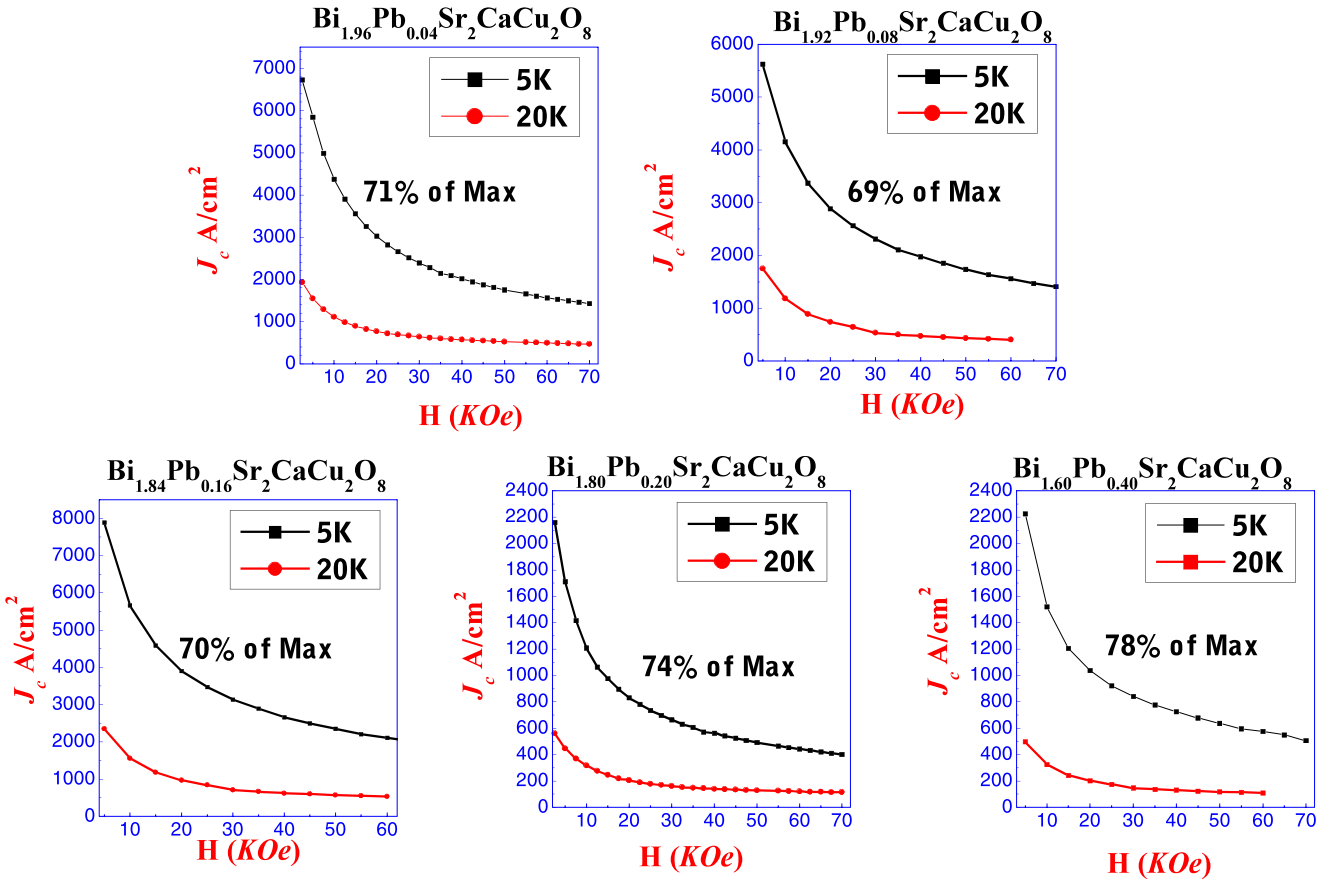
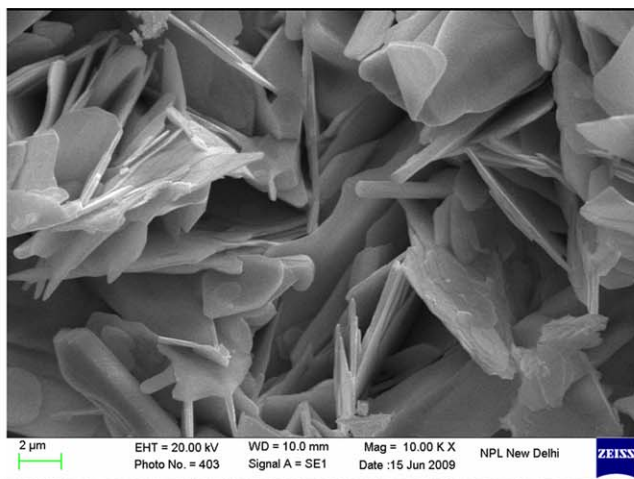
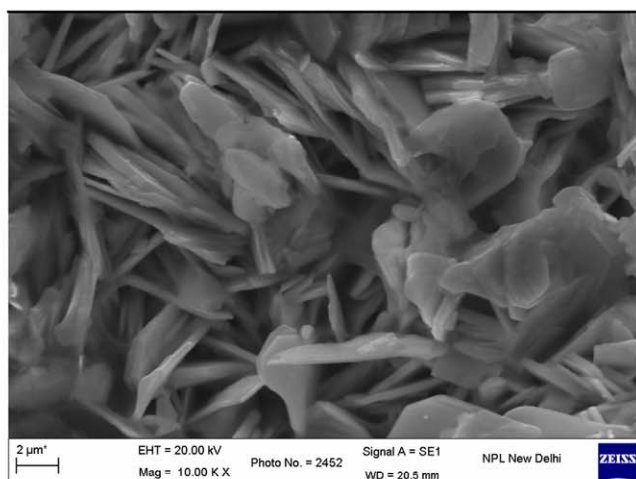
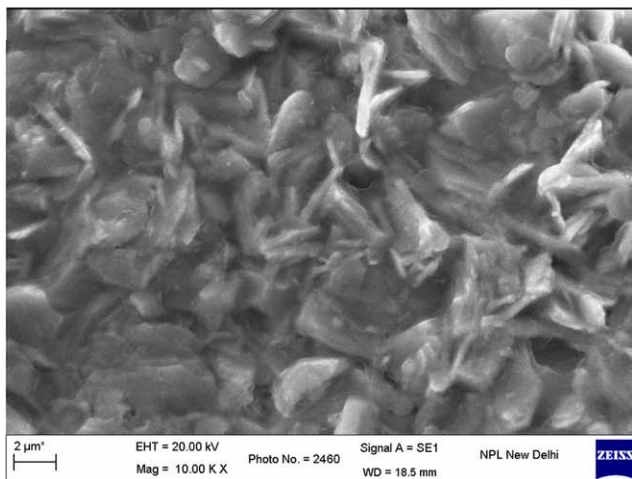
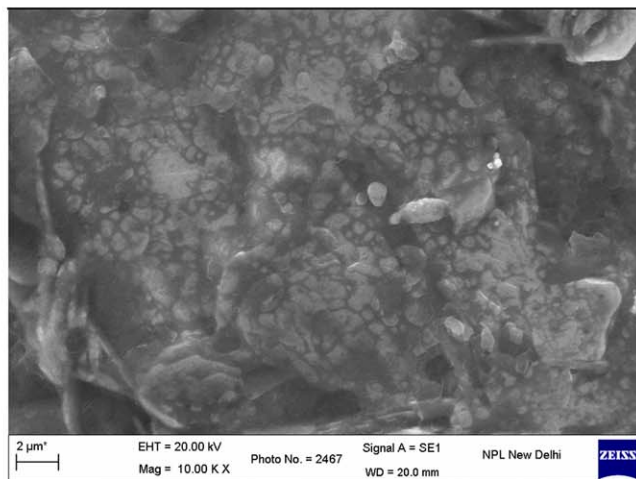
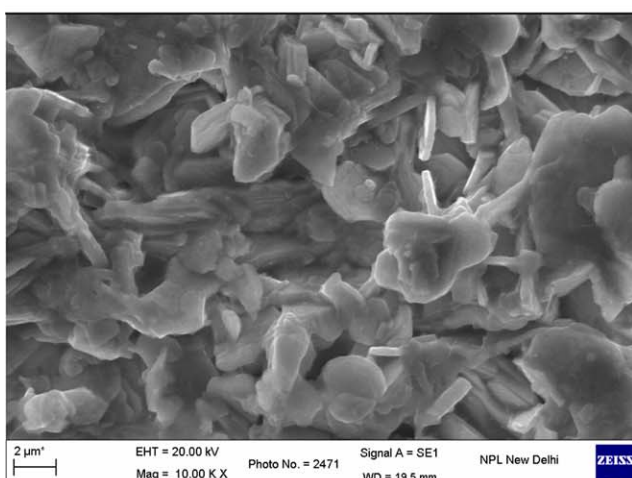
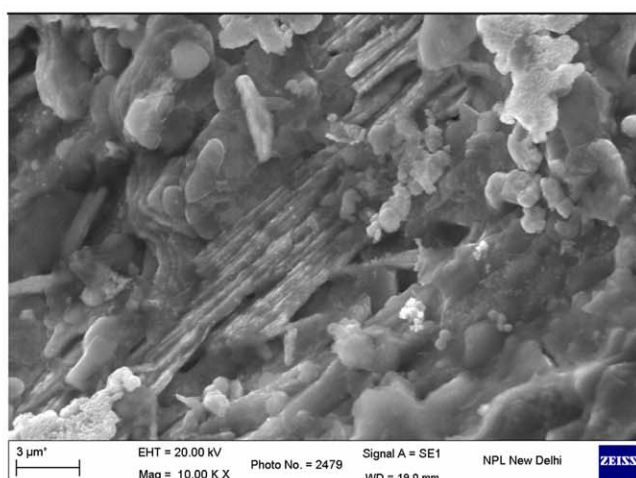


Fig. 6 J_c plots at 5 and 20 K for $\text{Bi}_{2-x}\text{Pb}_x\text{Sr}_2\text{CaCu}_2\text{O}_{8+\delta}$ ($x = 0$ to 0.4)

Fig. 7.1 $\text{Bi}_2\text{Sr}_2\text{Ca}\text{Cu}_2\text{O}_8$ Fig. 7.2 $\text{Bi}_{1.96}\text{PbO}_{0.04}\text{Sr}_2\text{Ca}\text{Cu}_2\text{O}_8$ Fig. 7.3 $\text{Bi}_{1.92}\text{PbO}_{0.08}\text{Sr}_2\text{Ca}\text{Cu}_2\text{O}_8$ Fig. 7.4 $\text{Bi}_{1.84}\text{PbO}_{0.16}\text{Sr}_2\text{Ca}\text{Cu}_2\text{O}_8$ Fig. 7.5 $\text{Bi}_{1.80}\text{PbO}_{0.20}\text{Sr}_2\text{Ca}\text{Cu}_2\text{O}_8$ Fig. 7.6 $\text{Bi}_{1.60}\text{PbO}_{0.40}\text{Sr}_2\text{Ca}\text{Cu}_2\text{O}_8$ Fig. 7 SEM micrographs of $\text{Bi}_{2-x}\text{Pb}_x\text{Sr}_2\text{Ca}\text{Cu}_2\text{O}_{8+\delta}$ ($x = 0$ to 0.4)

in $\text{Bi}_{1.80}\text{Pb}_{0.20}\text{Sr}_2\text{CaCu}_2\text{O}_8$ and $\text{Bi}_{1.60}\text{Pb}_{0.40}\text{Sr}_2\text{CaCu}_2\text{O}_8$ samples, as can also be seen in XRD plots.

All the results discussed above indicate the same outcome: that when we substitute the lead at bismuth site in $\text{Bi}_{2-x}\text{Pb}_x\text{Sr}_2\text{CaCu}_2\text{O}_8$ (Bi/Pb-2212), there is an overall improvement in superconducting properties of bulk samples up to $x = 0.16$ and then they start to degrade with a further increase in x .

4 Discussion

The characteristic $\langle 002 \rangle$ ($2\theta \approx 5.8^\circ$) and $\langle 200 \rangle$ ($2\theta \approx 47.5^\circ$) peaks in XRD plots were used to find the lattice parameters. Un-split $\langle 200 \rangle$ peaks are observed in all samples that ignore any structural distortion from tetragonal structure to orthorhombic structure. The calculated lattice parameters are given in Table 1. No significant change in lattice parameters was observed. The lengths of a - and b -axis are considered to be controlled by the in-plane Cu–O bond distance, which is closely related to the carrier concentration [14]. The a - and b -axis parameters should be decreased due to the increase in hole concentration, which can strengthen the Cu–O bonding force when Pb content increases [14]. Similarly, the c -axis parameter can change by the variation of oxygen content induced by aliovalent substitution. However, in our case no significant change has been observed in lattice parameters as the Pb content increases. This means that the effect of Pb doping on the microstructure of the Cu–O plane in Pb-substituted Bi-2212 is modest. The unchanged lattice parameters can be explained by two factors. One is the change in the oxygen content and second is the ionic size difference of Pb^{2+} and Bi^{3+} ions. The ionic size of Pb^{2+} ($R = 1.2 \text{ \AA}$) is considerably larger than that of Bi^{3+} ($R = 0.93 \text{ \AA}$). Thus, according to ionic size, the lattice parameters should increase with increase in Pb content. On the other hand, after doping Pb at the Bi-site, the valences of Cu and Bi, which are +2 and +3 respectively, are unchanged, while only the average valence of (Bi–Pb) decreases [15]. The difference in the valences between Pb^{2+} and Bi^{3+} lowers the extra oxygen content and decreases the lattice parameters. The opposite reaction of ionic size and ionic valence on lattice makes the substitution of Pb for Bi to have little effect on the structure of the samples, so that the average structures have no distinct change [16]. Thus, as a consequence of the structural change, the change in superconducting properties can be ruled out.

The practically important boundary in $H-T$ phase diagram is the irreversibility line (IL) which marks the boundary between the regions of reversible and irreversible magnetic behaviors with temperature. It is thought that the vortices are pinned by the defects in the crystals below irreversibility line, whereas they can move in responses to exter-

nal magnetic field above this line. Therefore, from the viewpoint of practical applications, it is particularly important to expand this irreversible regime to increase J_c . The splitting in FC and ZFC curves are thought to be caused by the screening currents running in superconductors. As has been observed from the magnetization vs. temperature plots and summarized in Table 1, the irreversible temperature T_{irr} increases towards higher temperature as is desirable for practical applications.

In the light of $R(T)$ plots, increased conductivity up to $x = 0.16$ can be attributed to the increase in charge carriers [5]. The increase of the charge carrier has been interpreted as a result of electron vacancy due to the additional holes contributed by the aliovalent Pb^{2+} ion replacing the trivalent Bi^{3+} . It was found by Calestani et al. [17] that the double (Bi, Pb) O layer plays a competitive role (with respect to the CuO_2 plane) in accommodating the extra charge deriving from the substitution of Pb^{2+} for Bi^{3+} . The bottom of the Bi–O bands lies below the Fermi energy E_F , allowing a transfer of electrons to occur from the CuO_2 planes to the double BiO planes and creating doping holes on the Cu–O bands [18]. Further, for $x > 0.16$, the decrease in conductivity can be explained on the basis of the effects arising from increase of porosity and secondary phases, and to the decrease of the grain alignment with increase in Pb content [12] as has been seen in SEM micrographs.

The optimization of J_c can be explained on the basis of a competition between the improved intra-granular superconductivity in $(\text{Bi}, \text{Pb})_2\text{Sr}_2\text{CaCu}_2\text{O}_8$ [5] and the degradation of bulk microstructure with increase in lead content [12]. Whereas, for the single crystals, the lead substitution increases the superconducting properties even up to $x = 0.4$. However, in case of bulk samples the superconducting properties start to deteriorate after $x = 0.16$ due to increase in porosity, poor grain connectivity, and growth of secondary phases. Thus, controlled substitution of lead in $\text{Bi}_2\text{Sr}_2\text{CaCu}_2\text{O}_8$ bulk system leads to optimization of its superconducting properties for $\text{Bi}_{1.84}\text{Pb}_{0.16}\text{CaCu}_2\text{O}_8$.

5 Conclusions

The effect of lead substitution at bismuth site has been studied in bulk Bi-2212. It is observed that there is a competition between improvement in intra-granular superconducting properties and the degradation in micro-structural properties of bulk. The resultant of the two is optimized superconducting properties for $x = 0.16$ in bulk $\text{Bi}_{2-x}\text{Pb}_x\text{Sr}_2\text{CaCu}_2\text{O}_8$.

Acknowledgements The authors thank NIMS Japan where the magnetization measurements were carried out. One of us (JKB) is further grateful to CSIR for financial help in terms of NET-JRF fellowship.

References

1. Tarascon, J.M., et al.: Phys. Rev. B **38**, 8885 (1988)
2. Cava, R.J.: Science **247**, 656 (1990)
3. Chen, C.H., Werder, D.J., Espinosa, G.P., Cooper, A.S.: Phys. Rev. B **39**, 4686 (1989)
4. Schneck, J., Pierre, L., Tolédano, J.C., Daguet, C.: Phys. Rev. B **39**, 9624 (1989)
5. Chong, I., Hiroi, Z., Izumi, M., Shimoyama, J., Nakayama, Y., Kishio, K., Terashima, T., Bando, Y., Takano, M.: Science **276**, 770 (1997)
6. Samanta, S.B., Dutta, P.K., Awana, V.P.S., Narlikar, A.V.: Euro. Phys. Lett. **16**, 391 (1991)
7. Awana, V.P.S., Samanta, S.B., Dutta, P.K., Gmelin, E., Narlikar, A.V.: J. Phys. Condens. Mater. **3**, 8893–8901 (1991)
8. Liang, J.K., et al.: Mod. Phys. Lett. B **2**, 483 (1988)
9. Torrance, J., et al.: Solid State Commun. **66**, 703 (1988)
10. Khan, Y.: J. Mater. Sci. Lett. **12**, 482–485 (1993)
11. Majewski, P., Su, H.L., Aldinger, F.: J. Mater. Sci. **31**, 2035 (1996)
12. Sotelo, A., Madre, M.A., Diez, J.C., Rasekh, S., Angurel, L.A., Martínez, E.: Supercond. Sci. Technol. **22**, 034012 (2009)
13. Bean, C.P.: Rev. Mod. Phys. **36**, 31 (1964)
14. Chen, X.H., Ruan, K.Q., Qian, G.G., Li, S.Y., Cao, L.Z., Zou, J., Xu, C.Y.: Phys. Rev. B **58**, 5868 (1998)
15. Hinnen, C., Nguyen van Huong, C., Marcus, P.: J. Electron Spectrosc. Relat. Phenom. **73**, 293 (1995)
16. Shi, L., Li, C., Dong, Q., Zhang, Y.: J. Phys. Condens. Mater. **13**, 5195–5204 (2001)
17. Calestani, G., Francesconi, M.G., Salsi, G., Andreetti, G.D., Migliori, A.: Physica C **197**, 283 (1992)
18. Chen, X.H., Ruan, K.Q., Qian, G.G., Li, S.Y., Cao, L.Z., Zou, J., Xu, C.Y.: Phys. Rev. B **58**, 5868 (1998)